A Protein Phosphorylation Switch at the Conserved Allosteric Site in GP

Kai Lin, Virginia L. Rath, Shirleko C. Dai, Robert J. Fletterick,* Peter K. Hwang*

A phosphorylation-initiated mechanism of local protein refolding activates yeast glycogen phosphorylase (GP). Refolding of the phosphorylated amino-terminus was shown to create a hydrophobic cluster that wedges into the subunit interface of the enzyme to trigger activation. The phosphorylated threonine is buried in the allosteric site. The mechanism implicates glucose 6-phosphate, the allosteric inhibitor, in facilitating dephosphorylation by dislodging the buried covalent phosphate through binding competition. Thus, protein phosphorylation-dephosphorylation may also be controlled through regulation of the accessibility of the phosphorylation site to kinases and phosphatases. In mammalian glycogen phosphorylase, phosphorylation occurs at a distinct locus. The corresponding allosteric site binds a ligand activator, adenosine monophosphate, which triggers activation by a mechanism analogous to that of phosphorylation in the yeast enzyme.

Reversible protein phosphorylation is a central mechanism in cellular regulation (*1–3*). Despite knowledge of the regulation and substrate specificity of protein kinases and phosphatases in cell signaling cascades, the structural basis of phosphorylation-initiated functional modification of proteins has been elucidated in only two instances: mammalian glycogen phosphorylase (GP) and *Escherichia coli* isocitrate dehydrogenase (IDH). IDH is inhibited by phosphorylation of a residue in the active site, which results in steric and electrostatic blocks to substrate binding (*4*). Mammalian GP is activated by a phosphorylation-mediated protein conformational change, which is the result of ionic interactions of the covalent phosphoryl group pulling the enzyme subunits together (*5–8*). These distinct mechanisms provide limited information on the principles by which protein phosphorylation operates and evolves. We therefore examined the phosphorylation mechanism that regulates yeast (*Saccharomyces cerevisiae*) GP. In yeast and mammalian GPs, dissimilar reversible phosphorylation switches turn on and off a common catalytic machinery that converts glycogen into glucose 1-phosphate to provide energy (*9*). We compared the crystal structure of a phosphorylated, active form of yeast GP with the structure of the unphosphorylated, inactive enzyme (*10*). The differences revealed a phosphoregulatory mechanism with an evolutionary relation to that of the mammalian homolog, as well as regulatory and evolutionary principles that could apply to a wide range of cellular phosphoproteins.

Yeast GP is translated as an inactive enzyme and can be activated only through phosphorylation of a threonine residue within a 39–amino acid NH_2-terminal extension relative to the NH_2-terminus of the mammalian enzyme (*11, 12*). In the structure of the unphosphorylated enzyme complexed with the allosteric inhibitor glucose 6-phosphate (Glc-6-P), the NH_2-terminal extension of each subunit binds near the catalytic site of the neighboring subunit in the homodimer (Fig. 1A) (*10*). The phosphorylation site, Thr^{-10} (residues are numbered −1 to −39 toward the NH_2-terminus relative to the mammalian GP NH_2-terminus), is located in a nonpolar region near the dimer interface. These observations led to the proposal that phosphorylation activates the enzyme solely by displacing the NH_2-terminus to relieve a steric block of the catalytic site. However, a molecule with 22 NH_2-terminal residues deleted is inactive (*13*). This enzyme variant, Nd22, still requires phosphorylation for activation and exhibits properties identical to those of the native enzyme. Thus, activation apparently requires a more active role for the NH_2-terminal region.

We have now determined the crystal structure of the phosphorylated form of Nd22 at 2.8 Å resolution (Fig. 1B). The crystallographic data and refinement statistics are shown in Table 1 (*14*). Compared with the structure of the unphosphorylated enzyme, there is a progressive increase in subunit-to-subunit separation from the regulatory face to the catalytic face (*15*). This displacement of subunits is accompanied by a reorientation of the symmetrically disposed "tower" (residues

Table 1. Crystal parameters, crystallographic data, and refinement statistics for the phosphorylated Nd22 yeast GP. The space group is $P2_12_12_1$. Cell constants are a = 103.91 Å, b = 143.93 Å, c = 169.26 Å, and $\alpha = \beta = \gamma = 90°$. The asymmetrical unit contains the functional dimer. The structure was determined by molecular replacement with X-PLOR (*27*). The search model consists of residue 20 to the COOH-terminus of the unphosphorylated yeast GP monomer. The orientation of one subunit was determined in a cross-rotation search procedure with data from 10 to 4 Å resolution and vectors from 15 to 45 Å. Translation search of the correctly orientated monomer, with data from 10 to 4 Å resolution, produced a correlation peak 21σ greater than the mean and 9σ greater than the next peak. The orientation and translation of the second subunit were determined through identifying the twofold noncrystallographic symmetry operator with the self-rotation function, followed by translation search. The structure was refined by rigid-body, positional, and simulated-annealing refinement protocols implemented in X-PLOR. The noncrystallographic symmetry operator was imposed during refinement. Model rebuilding was performed with CHAIN (*28*).

Parameter	Value
Data statistics	
No. of reflections measured (2σ cutoff)	247,322
No. of unique reflections	50,707
R_{merge}* (%)	10.5
Completeness to 2.8 Å (%)	72
Completeness between 2.8 and 3.0 Å (%)	43
Refinement statistics	
No. of atoms	8233
R_{cryst}† (6.0–2.8 Å) (%)	17.9
R_{free}‡ (6.0–2.8 Å) (%)	23.9
rms§ deviation from ideal	
Bond lengths (Å)	0.018
Bond angles (degrees)	2.87

*$R_{merge} = \Sigma_h \Sigma_i | I(h) - I_i(h) | / \Sigma_h \Sigma_i I_i(h)$, where $I_i(h)$ and $I(h)$ are the ith and the mean measurement of the intensity of reflection, h, respectively. †$R_{cryst} = \Sigma_h [|F_o(h) - F_c(h)|] / \Sigma_h F_o(h)]$, where $F_o(h)$ and $F_c(h)$ are the observed and calculated structure factor amplitudes, respectively. ‡R_{free} was calculated from 10% of the data chosen randomly and omitted from the refinement. §rms, root mean square.

K. Lin, S. C. Dai, R. J. Fletterick, P. K. Hwang, Department of Biochemistry and Biophysics, University of California at San Francisco, 513 Parnassus, San Francisco, CA 94143, USA.
V. L. Rath, Central Research Division, Pfizer Inc., Groton, CT 06340, USA.
*To whom correspondence should be addressed.

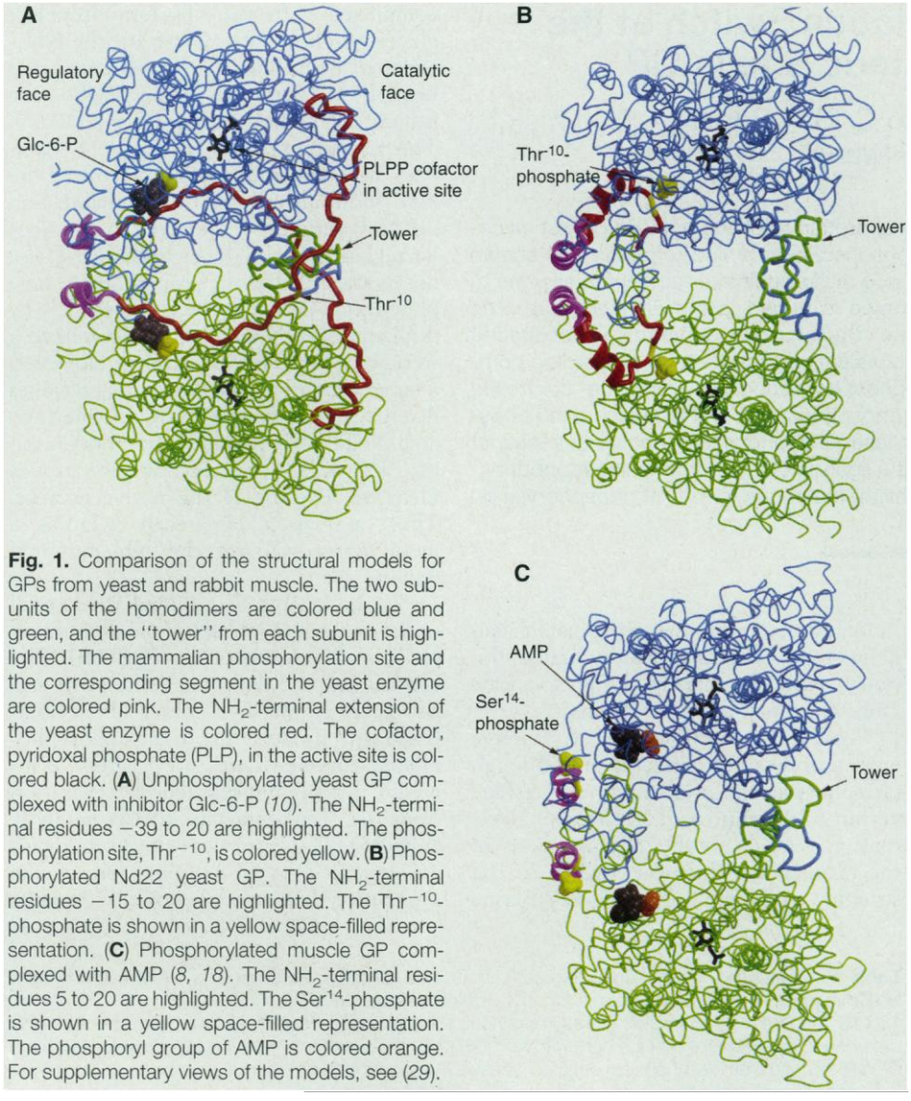

Fig. 1. Comparison of the structural models for GPs from yeast and rabbit muscle. The two subunits of the homodimers are colored blue and green, and the "tower" from each subunit is highlighted. The mammalian phosphorylation site and the corresponding segment in the yeast enzyme are colored pink. The NH_2-terminal extension of the yeast enzyme is colored red. The cofactor, pyridoxal phosphate (PLP), in the active site is colored black. (**A**) Unphosphorylated yeast GP complexed with inhibitor Glc-6-P (*10*). The NH_2-terminal residues −39 to 20 are highlighted. The phosphorylation site, Thr^{-10}, is colored yellow. (**B**) Phosphorylated Nd22 yeast GP. The NH_2-terminal residues −15 to 20 are highlighted. The Thr^{-10}-phosphate is shown in a yellow space-filled representation. (**C**) Phosphorylated muscle GP complexed with AMP (*8*, *18*). The NH_2-terminal residues 5 to 20 are highlighted. The Ser^{14}-phosphate is shown in a yellow space-filled representation. The phosphoryl group of AMP is colored orange. For supplementary views of the models, see (*29*).

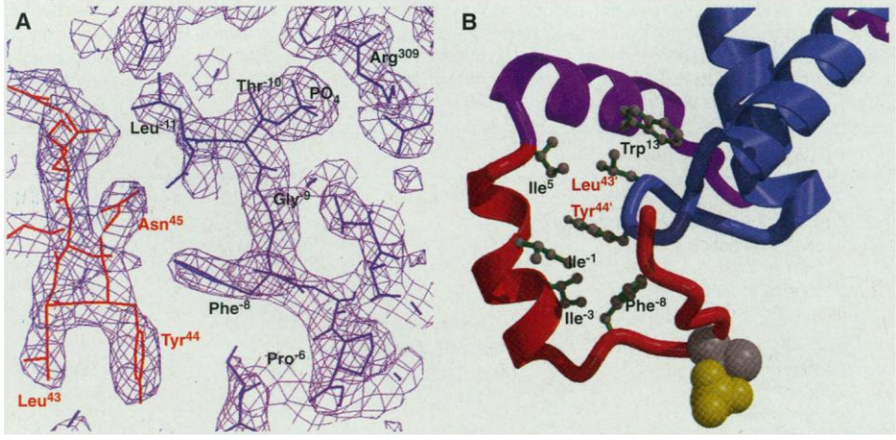

Fig. 2. (**A**) The $2F_o - F_c$ electron density map of the phosphorylated NH_2-terminal region of Nd22 yeast GP contoured at 1.2σ. One subunit is colored purple, and the symmetry-related subunit is colored orange. (**B**) Hydrophobic interactions between the phosphorylated NH_2-terminus and the CAP region of the neighboring subunit. The NH_2-terminal hydrophobic side chains are labeled black, and the hydrophobic side chains from the CAP region are labeled red. The Thr^{-10}-phosphate is shown in a space-filled representation with the phosphoryl group colored yellow.

261 to 274) near the catalytic face. Within each subunit, there is a smaller increase in the separation between opposing NH_2-terminal and COOH-terminal domains that form the catalytic cleft. A detailed analysis of these movements will be presented elsewhere (*16*).

We located all but the two most NH_2-terminal residues (−16 and −17) of Nd22 in the electron density map (Fig. 2A). This region differs from its stretched-out conformation in the unphosphorylated structure. A region of 12 residues, from position 5 to −7, contracts to form a three-turn amphipathic helix (Fig. 2B). The eight residues from position −8 to −15, including the phosphorylated Thr^{-10}, form a hairpin-like structure that docks into the deep crevice between the subunits. The Thr^{-10}-phosphate is coordinated by the side chains of Arg^{309} and Arg^{310}, the same components identified in binding the phosphoryl group of the inhibitor Glc-6-P in the unphosphorylated structure. The rearrangement of residues 5 to −15 is stabilized by a clustering of hydrophobic side chains from the NH_2-terminus (Phe^{-8}, Ile^{-3}, Ile^{-1}, Ile^{5}, and Trp^{13}) and from the "CAP" loop (residues 42 to 46) of the neighboring subunit (Leu^{43} and Tyr^{44}).

The mammalian GP phosphorylation site is distinct (*17*). Moreover, the mammalian GP can be independently activated by phosphorylation of Ser^{14} or binding of adenosine monophosphate (AMP) (*18–20*). The key features of the mammalian GP activation mechanism are shown in the structure of the phosphorylated rabbit muscle enzyme complexed with AMP (Fig. 1C) (*6–8*, *18*). On phosphorylation, the NH_2-terminal tail changes conformation from a mostly β structure to a partially coiled helical structure comparable to the corresponding region of both the unphosphorylated and phosphorylated yeast enzyme. The Ser^{14}-phosphate from each subunit binds in a shallow groove at the dimer interface, forming ionic contacts with the side chains of Arg^{69} from the same subunit and of Arg^{43} from the CAP region of the symmetry-related subunit. The alternative activator, AMP, binds in a deeper crevice between the subunits, with its phosphoryl group 12 Å away from the binding site of the Ser^{14}-phosphate. The binding of activator AMP and that of inhibitor Glc-6-P are mutually exclusive because the phosphoryl groups of both effectors pair with the same residues of GP, Arg^{309} and Arg^{310}. Activation by AMP is mediated by a hydrophobic stacking interaction between the adenine ring and the side chain of Tyr^{75} (*8*, *18*).

The mechanisms that trigger activation by phosphorylation in yeast and mamma-

lian GPs differ in fundamental character (Fig. 3). The mammalian trigger is mainly ionic in origin—phosphorylation of Ser^{14} introduces new charge-to-charge interactions, which pull subunits together. Sulfate can trigger activation by forming the same bridging ionic interactions (*20, 21*). Activation can also be mimicked with designed metal binding sites to achieve the pulling (*22*). In the yeast GP, triggering of activation by phosphorylation cannot be accounted for by new charge-to-charge interactions, because Thr^{-10}-phosphate substitutes at the binding site of the phosphoryl group of the inhibitor. Binding of Thr^{-10}-phosphate functions to bring activation elements, composed of hydrophobic residues surrounding the phosphorylation site, into suitable juxtaposition. In this manner, phosphorylation induces a localized protein folding of a miniature hydrophobic core that perturbs the dimer interface and causes activation. Despite divergence in activation by phosphorylation, there is mechanistic resemblance between activation by phosphorylation in the yeast GP and activation by AMP in mammalian GP (Fig. 3). In addition to operating at the same locus, both mechanisms rely on hydrophobic interactions and require their respective activating agents to bridge identical structural elements across the dimer interface—the CAP loop of one subunit and the phosphate binding pocket of the neighbor.

The structural consequence of phosphorylation in yeast GP, reinforced by the mechanisms of phosphorylation in *Escherichia coli* IDH and mammalian GP, reveals a general level of control over the reversible phosphorylation cycle through the action of facilitators of phosphorylation or dephosphorylation. The mechanism for each of the three enzymes reveals that the covalent phosphoryl group is anchored through an intramolecular binding event. The binding is important not only in maintaining functional modification of the protein, but also in protecting the phosphoryl group from phosphatase to prevent a futile phosphorylation-dephosphorylation cycle. However, this energetically favorable binding event must be reversed so that dephosphorylation can proceed. The mechanism of yeast GP suggests that Glc-6-P serves as a dephosphorylation facilitator by modifying accessibility of the phosphorylation site to protein phosphatase (*23*). A high concentration of intracellular Glc-6-P signals ample energy and promotes dephosphorylation of yeast GP by binding competitively to dislodge the buried phosphorylated peptide. A similar control mechanism regulates mammalian GP, but in this instance, glucose is the high-energy signal. The binding of glucose at the active site of muscle GP induces a structural change that destabilizes the binding of the Ser^{14}-phosphate within the subunit interface 30 Å away, facilitating its accessibility to protein phosphatase (*24*). Regulatory features that facilitate phosphorylation can have an equally important role. Glycogen serves as a facilitator of phosphorylation of yeast GP by shifting the enzyme from a tetrameric to a dimeric state (*13*). Analogously, cyclin A facilitates phosphorylation of cyclin-dependent protein kinase by rendering the phosphorylation site more accessible (*25*). Modifying accessibility of the phosphorylation site to protein kinases and phosphatases through specific facilitators may be a common second level of regulation of reversible phosphorylation cycles. It establishes the potential for both intracellular and extracellular regulatory signals to be processed by the target protein.

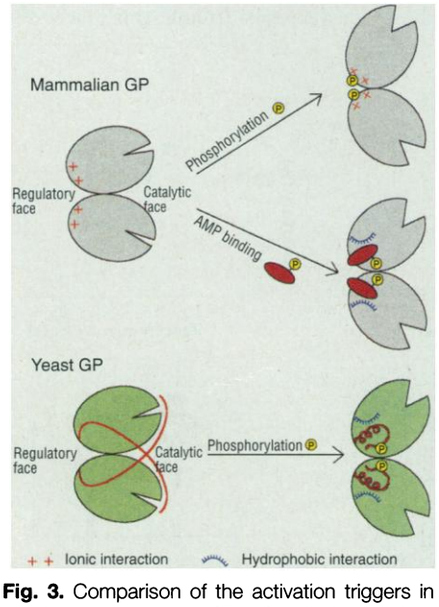

Fig. 3. Comparison of the activation triggers in yeast and mammalian GPs. See text for further details.

Given that inhibition by Glc-6-P appears to have evolved before phosphorylation control (*26*), reversible phosphorylation in yeast GP probably evolved by taking advantage of the existing binding pocket for the phosphoryl ligand. It is possible that the ancestral enzyme did not require phosphorylation for activity and that phosphorylation simply prohibited Glc-6-P inhibition by blocking the site. The role of phosphorylation may then have shifted from an anti-inhibitor to an obligate activator, with the unphosphorylated enzyme being a catalytically inactive form. Such a progression from a ligand binding pocket to a phosphorylation control mechanism may be advantageous because phosphorylation offers an immediate functional effect through binding competition with the ligand. These evolutionary steps further ensure a simultaneous control on dephosphorylation with the ligand as a facilitator.

REFERENCES AND NOTES

1. P. Cohen, *Eur. J. Biochem.* **151**, 439 (1985).
2. E. G. Krebs, in *The Enzymes*, P. D. Boyer and E. G. Krebs, Eds. (Academic Press, New York, 1986), vol. 17, pp. 3–20.
3. H. V. Rickenberg and B. H. Leichtling, in *ibid.*, vol. 18, pp. 419–455.
4. R. M. Stroud, *Curr. Opin. Struct. Biol.* **1**, 826 (1991).
5. L. N. Johnson, and D. Barford, *Protein Sci.* **3**, 1726 (1994).
6. S. R. Sprang *et al.*, *Nature* **336**, 215 (1988).
7. D. Barford and L. N. Johnson, *ibid.* **340**, 609 (1989).
8. D. Barford *et al.*, *J. Mol. Biol.* **218**, 233 (1991).
9. P. K. Hwang and R. J. Fletterick, *Nature* **324**, 80 (1986).
10. V. Rath and R. J. Fletterick, *Nature Struct. Biol.* **1**, 681 (1994).
11. M. Fosset, L. W. Muir, L. D. Nielsen, E. H. Fisher, *Biochemistry* **10**, 4105 (1971).
12. K. Lerch and E. H. Fischer, *ibid.* **14**, 2009 (1975).
13. K. Lin, P. K. Hwang, R. J. Fletterick, *J. Biol. Chem.* **270**, 26833 (1995).
14. The procedures for the purification and phosphorylation of yeast GP were as previously described (*13*). The details of crystallization and structure determination will be presented elsewhere (*16*).
15. The GP dimer has been functionally described as having two "faces": the regulatory face, at which allosteric effectors and the phosphorylated NH_2-termini bind, and the catalytic face, on the opposite side, where the substrates enter.
16. K. Lin, P. K. Hwang, R. J. Fletterick, in preparation.
17. The phosphorylation site sequences of the mammalian and yeast GPs are Lys-Arg-Lys-Gln-Ile-Ser^{14}-Val-Arg-Gly and Leu-Thr-Arg-Arg-Leu-Thr^{-10}-Gly-Phe-Leu, respectively, where the residues undergoing reversible phosphorylation are numbered. The yeast GP is efficiently phosphorylated by a cyclic adenosine 3′,5′-monophosphate–dependent protein kinase, whereas the mammalian GP is recognized by a highly specific GP kinase [D. J. Graves, *Methods Enzymol.* **99**, 268 (1983)].
18. S. Sprang, E. Goldsmith, R. Fletterick, *Science* **237**, 1012 (1987).
19. E. J. Goldsmith, S. R. Sprang, R. Hamlin, N.-H. Xuong, R. J. Fletterick, *ibid.* **245**, 528 (1989).
20. L. N. Johnson, *FASEB J.* **6**, 2274 (1992).
21. D. D. Leonidas *et al.*, *FEBS Lett.* **261**, 23 (1990).
22. M. F. Browner, D. Hackos, R. J. Fletterick, *Nature Struct. Biol.* **1**, 317 (1994).
23. Glc-6-P inhibits the phosphorylated yeast GP cooperatively (*13*). The crystal structure of the phosphorylated yeast GP complexed with Glc-6-P revealed that Glc-6-P displaces the Thr^{-10}-phosphate from the binding site completely. The NH_2-terminus becomes disordered in that structure (K. Lin *et al.*, in preparation).
24. W. Stalmans, H. DeWulf, B. Lederer, H. G. Hers, *Eur. J. Biochem.* **15**, 9 (1970).
25. P. D. Jeffrey *et al.*, *Nature* **376**, 313 (1995).
26. J. W. Hudson, G. B. Golding, M. M. Crerar, *J. Mol. Biol.* **234**, 700 (1993).
27. A. Brunger, *X-PLOR, Version 3.1* (Yale Univ. Press, New Haven, CT, 1992).
28. J. S. Sack, *J. Mol. Graphics* **6**, 244 (1988).
29. Supplementary information is available at the authors' Web site: http://util.ucsf.edu/flett/lin/science.html.

30. We thank I. Herskowitz, A. Weiss, M. M. Crerar, and S. L. Slatin for critical reading and discussion of the manuscript, and D. Singler for the art work. Supported by NIH grant DK32822 to R.J.F. K.L. is a Burroughs Wellcome Fund Fellow of the Life Sciences Research Foundation.

11 March 1996; accepted 24 June 1996